Cement and Concrete Research 41 (2011) 1112–1122

Contents lists available at ScienceDirect

Cement and Concrete Research

journal homepage: http://ees.elsevier.com/CEMCON/default.asp

Thermal and mechanical properties of fiber reinforced high performance self-consolidating concrete at elevated temperatures

Wasim Khaliq, Venkatesh Kodur *

Department of Civil and Environmental Engineering, 3546 Engineering Building, Michigan State University, East Lansing, MI 48824-1226, United States

ARTICLE INFO

Article history:
Received 14 December 2010
Accepted 24 June 2011

Keywords:
Self-consolidating concrete
Temperature (A)
Mechanical properties (C)
Thermal analysis (B)
Fiber reinforcement (E)

ABSTRACT

This paper presents the effect of temperature on thermal and mechanical properties of self-consolidating concrete (SCC) and fiber reinforced SCC (FRSCC). For thermal properties specific heat, thermal conductivity, and thermal expansion were measured, whereas for mechanical properties compressive strength, tensile strength and elastic modulus were measured in the temperature range of 20–800 °C. Four SCC mixes, plain SCC, steel, polypropylene, and hybrid fiber reinforced SCC were considered in the test program. Data from mechanical property tests show that the presence of steel fibers enhances high temperature splitting tensile strength and elastic modulus of SCC. Also the thermal expansion of FRSCC is slightly higher than that of SCC in 20–1000 °C range. Data generated from these tests was utilized to develop simplified relations for expressing thermal and mechanical properties of SCC and FRSCC as a function of temperature.

1. Introduction

In the last three decades, there has been significant improvement in concrete technology and this has lead to development of high performing concretes such as, high performance concrete (HPC), self consolidating concrete (SCC), and fly ash concrete (FAC). SCC is a highly workable, non-segregating concrete that can easily reach into remote corners, fill congested formworks and reinforcement without any vibration efforts [1]. SCC application was mainly in bridges, underwater and heavily reinforced concrete structures in the last two decades. In recent years, the use of SCC has been extended to buildings construction. When used in building applications, structural members made of SCC have to satisfy fire resistance requirements specified in building codes, since fire represents one of the most severe environmental conditions to which structures may be subjected.

SCC was specifically developed by altering conventional mix design to obtain high fluidity and cohesiveness [1] so as to flow under its own weight without segregation. The changes in mix design include low water cement ratio and large dosage of chemical admixtures which produce higher compressive strength in SCC with dense microstructure [1]. The characterization of SCC with finer pore distribution and poor pore connectivity resembles that of high strength concrete (HSC) [1]. Recent fire resistance studies have clearly indicated that HSC has lower fire performance (due to strength loss and explosive spalling) as compared to conventional normal strength concrete (NSC) [2,3]. Therefore, it is envisaged in the literature that SCC due to similar strength and compactness as that of HSC has lower fire resistance properties as that of HSC.

Evaluating fire resistance of a structural system requires knowledge of high temperature properties of constituent materials. The properties of SCC that are needed for fire resistance analysis are thermal, mechanical, deformation properties, and material specific phenomenon such as fire induced spalling in concrete. Thermal properties include thermal conductivity, specific heat, thermal diffusivity, thermal expansion and mass loss. Deformation properties such as creep and mechanical properties such as strength, deformation, and elastic modulus significantly influence the fire response of a structural system. In addition, fire induced spalling which occurs in HSC under certain conditions can alter the response of a reinforced concrete structural system [1,4,5]. In HSC structural members, fibers are often added to overcome the adverse effects of fire induced spalling. Since high strength SCC has similar characteristics as that of HSC, it is also prone to fire induced spalling, therefore use of different fibers, such as steel and polypropylene fibers, is also proposed in SCC [1]. Although limited information is available on high temperature mechanical properties of SCC [6,7], very limited data is available on high temperature thermal properties of fiber reinforced SCC (FRSCC).

The aim of this study is to evaluate high temperature thermal and mechanical properties of high performing SCC and FRSCC. Thermal properties consisting of specific heat, thermal conductivity, and thermal expansion and mechanical properties consisting of compressive strength, tensile strength, and elastic modulus were measured. All properties except for thermal expansion were measured in the temperature range of 20–800 °C, while thermal expansion measurements were carried out in the temperature range of 20–1000 °C. Data generated from tests was utilized to develop simplified relations for

* Corresponding author. Tel.: +1 517 353 9813; fax: +1 517 432 1827.
E-mail addresses: khaliqwa@msu.edu (W. Khaliq), kodur@egr.msu.edu (V. Kodur).

0008-8846/$ – see front matter © 2011 Elsevier Ltd. All rights reserved.
doi:10.1016/j.cemconres.2011.06.012

expressing thermal and mechanical properties of SCC and FRSCC as a function of temperature.

2. High temperature properties of SCC

2.1. General

For predicting fire response of SCC structures, both temperature profiles in the cross section and strength degradation resulting from higher temperatures, are needed as function of temperature. For evaluating such temperature profiles and strength degradation with temperature, high temperature properties of SCC are needed.

2.2. Thermal properties

Concrete contains moisture in different forms and at high temperature this moisture evaporates at different rates. This leads to physical and chemical changes in microstructure phenomenon and thus influences the variation of thermal conductivity with temperature. Thermal conductivity is usually measured by means of 'steady state' or 'transient' test methods. Transient methods are preferred to measure thermal conductivity of moist concrete over steady-state methods [8,9], as physiochemical changes of concrete at higher temperatures cause unsteady heat flow. The thermal conductivity of conventional NSC and HSC, at room temperature, ranges between 2.3 and 2.8 W/m-°C [10]. But there is limited information on thermal conductivity of SCC and FRSCC in literature.

Specific heat of concrete is highly influenced by moisture content, aggregate type, and density of concrete [11–13]. Generally for HSC the specific heat remains constant up to 400 °C however it increases beyond 400 °C as more heat is required to release the chemically bound moisture in concrete [14]. The variation in specific heat at elevated temperatures is mainly attributed to moisture content, type of aggregate, test conditions and measurement techniques used in experiments [8,9]. No previous studies have been reported on specific heat of SCC and FRSCC.

Linear thermal expansion is the thermal strain resulting from increased temperature. Thermal expansion of concrete is generally influenced by cement type, water content, aggregate type, temperature and age [8]. Fig. 1 illustrates the variation of thermal expansion in SCC as a function of temperature as reported by Uygunoğlu [15]. It can be observed that there is significant variation in thermal expansion of SCC with different water cement ratios. This variation of thermal expansion is a function of concrete mix ingredients, moisture content, and aggregate type. Thermal expansion is an important property to predict the thermal stresses introduced to structural member under fire conditions.

2.3. Mechanical properties

Compressive strength of concrete depends upon water–cement ratio, aggregate–paste interface transition zone, curing conditions, aggregate type and size, admixture types and type of stress [16]. Unlike high temperature thermal properties, some investigations are available on high temperature compressive strength of SCC. Fig. 2 illustrates ratio of compressive strength at specified temperature to that at room temperature ($f'_{c,T}/f'_c$) as a function of temperature for SCC compiled from different references [1,5,7,17]. The reported data is based on residual compressive strength tests except that from Persson [7] that was done under unstressed state. There is difference between residual and unstressed test as these represent different scenarios to which concrete can be subjected. While unstressed method simulates the behavior of concrete in a structure under fire, residual test simulates the scenario of a concrete element cooled after exposure to fire. The strength gain between 100 and 300 °C is observed by Fares [17] which is attributed to rehydration of the desiccated matrix at early temperatures. This observation has also been reported by Dias [18] for HSC. The reduction in compressive strength with temperature observed by Persson is gradual without any spikes. It can be observed that the strength trends of SCC are not consistent and there are significant variations in strength loss, as reported by various authors.

The tensile strength of concrete is often neglected in strength calculations at room and elevated temperature. However it is an important property, because cracking in concrete is generally due to tensile stresses and the structural damage of the member in tension is often generated by progression in microcracks [19]. Tensile strength of concrete is dependent on almost same factors as compressive strength of concrete. Addition of fibers such as steel fibers does enhance the tensile strength of concrete [20]. Under fire conditions tensile strength of concrete can be even more crucial in cases where fire induced spalling occurs in a concrete structural member. The fire induced spalling is dependent on a number of factors including, permeability of concrete, type of fire exposure, and tensile strength of concrete [4,21]. Higher tensile strength can help in minimizing spalling [22]. Thus information on temperature dependent tensile strength of concrete is crucial for predicting fire induced spalling in concrete members.

Fig. 3 illustrates ratio of splitting tensile strength at specified temperature to that at room temperature ($f'_{t,T}/f'_t$) of SCC as a function of temperature as reported in two previous studies [5,23]. It can be seen that only limited measurements (up to 600 °C in one study and up to 330 °C in the second study) were made. The loss in tensile strength is steeper in comparison to gradual loss in compressive strength as reported by Sideris [5]. The rapid loss of tensile strength in HSC's is attributed to the development of microcracks as a result of thermal incompatibility within concrete and this has also been reported by Chan [19] and Khoury [24]. However, like compressive

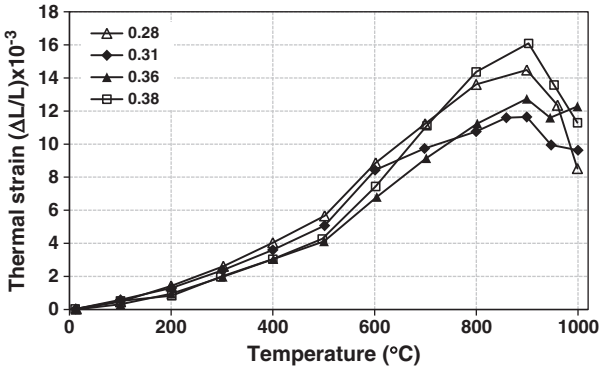

Fig. 1. Variation in thermal expansion of SCC as a function of temperature.

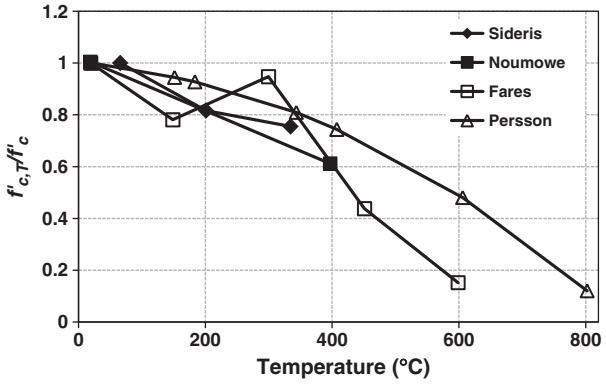

Fig. 2. Variation in relative compressive strength of SCC as function of temperature.

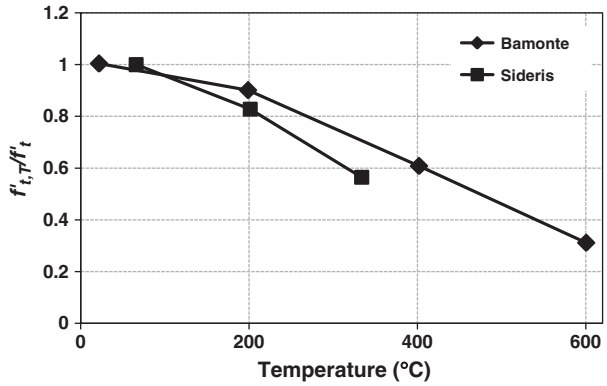

Fig. 3. Variation in relative splitting tensile strength of SCC as function of temperature.

strength, there is much variation observed in tensile strength of SCC. As there is very limited data available on high temperature splitting tensile strength of SCC and FRSCC this variation cannot be explained. The effect of temperature on tensile strength of SCC becomes more pronounced at higher temperatures as development of pore pressure in dense micro-structured high performing SCC causes rapid loss of tensile strength.

Another property that influences fire response of concrete structures is the elastic modulus of concrete which decreases with temperature. At high temperatures, disintegration of hydrated cement products and breakage of bonds in microstructure of cement paste reduces elastic modulus and the extent of reduction depends on moisture loss, high temperature creep and type of aggregate. Fig. 4 illustrates the ratio of elastic modulus at target temperature $E_{c,T}$ to elastic modulus at room temperature E_c as a function of temperature for SCC as reported in two studies [23,25]. It can be observed that there is excessive loss of elastic modulus of SCC with temperature. This lower modulus can be attributed to the excessive thermal stresses and physical and chemical changes in concrete microstructure. No data is available on elastic modulus of FRSCC in literature.

2.4. Fire induced spalling

Spalling is one of the major concerns with dense micro-structured concretes that occur when exposed to rapidly rising temperatures encountered in fire. Since high strength SCC has similar microstructure as that of HSC, SCC is also susceptible to risk of spalling. Low permeability associated with dense microstructure of concrete prevents dissipation of water vapors produced because of heat and leads to buildup of high pore pressure. When this fire induced pore pressure exceeds the tensile strength of concrete, which decreases with temperature, spalling occurs. Thus tensile strength plays an important role in minimizing or delaying spalling at elevated temperatures. Previous studies have shown that spalling in HSC is affected by concrete strength, permeability, concrete density, moisture content, fire intensity, presence of fibers and specimen dimensions [22,26].

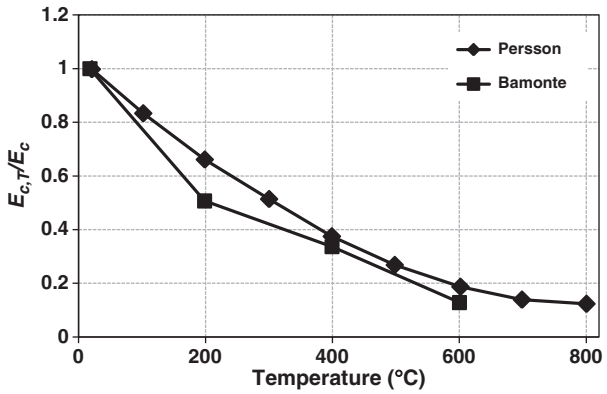

Fig. 4. Variation in elastic modulus of SCC with temperature.

To mitigate fire induced spalling in HSC, researchers have recommended addition of polypropylene fibers in concrete [21]. Polypropylene fibers melt at relatively low temperatures (about 167–170 °C) and create randomly oriented micro and macro channels inside concrete [27]. These channels facilitate dispersion of high vapor pressure. Another approach to overcome the spalling is through enhancing tensile strength of HSC by addition of steel fibers [28]. To optimize the solutions for spalling mitigation, the use of hybrid fibers in HSC has also been recommended, where both steel and polypropylene fibers are added in concrete mix [4,29]. For applying numerical models for predicting spalling in SCC or FRSCC reinforced concrete member, high temperature thermal and mechanical properties are needed.

The above review on high temperature properties of SCC indicates that only limited information is available on compressive strength; however, no reliable data is available on thermal properties, splitting tensile strength and elastic modulus of SCC and FRSCC. Moreover, data on reported high temperature properties of SCC shows large variations that can be attributed to investigation factors such as different test methods, mix proportions, test techniques, test conditions and heating regimes adopted by different researchers [5,30].

3. Test program

To develop high temperature thermal and mechanical properties for SCC, a comprehensive test program was undertaken on four types of SCC namely, SCC, SCC reinforced with steel (SCC-S), polypropylene (SCC-P), and hybrid fibers (SCC-H). Data generated from tests was utilized to characterize the high temperature properties of SCC to that of FRSCC.

3.1. Mix proportions and test specimens

A total of four batches of concrete involving SCC, SCC-S, SCC-P, and SCC-H were prepared for fabricating test specimens. These mixes had ordinary Portland cement (Type I), limestone (carbonate) based coarse aggregate of maximum size 10 mm, and natural source sand fine aggregate. To achieve desired strength and workability properties, optimum amount of mineral admixtures, such as slag and fly ash (Class C), was added to batch mix.

For fiber reinforced SCC mixes, commercially available fibers, NOVOCON XR type steel fibers and MONOFILAMENT (multi-plus) type polypropylene fibers were added. Steel fibers in FRSCC mix were 38 mm in length and 1.14 mm equivalent diameter and had a specified tensile strength of 966 MPa. Polypropylene fibers in FRSCC were nonabsorbent type with 20 mm length, 0.91 specific gravity and 162 °C melting point. Steel fibers in SCC-S were 42 kg/m^3 of concrete representing 1.75% by mass. Polypropylene fibers in SCC-P were 1 kg/m^3 representing 0.05% by mass. In the case of SCC-H the proportion of steel and polypropylene fibers were 42 kg/m^3 steel, and 1 kg/m^3 polypropylene, representing 1.75% and 0.05% by mass respectively.

A total of twelve, 100×200 mm and thirty-six, 75×150 mm cylinders were fabricated for undertaking compressive and splitting tensile strength tests on each type of concrete (see Table 1). For thermal properties, two, 100×100×300 mm prism specimens were fabricated for each concrete. The specimens were demolded one day after casting and cured under controlled conditions of 95% humidity and 20 °C temperature. 25% of 75×150 mm cylinders were instrumented with type K thermocouples, one placed at center and another placed on surface. The instrumented cylinders were used as control specimens to determine the time required to attain a target temperature under steady state conditions. Compression tests were conducted using 100×200 mm cylinders at 7, 28 and 90 days after casting of the

Table 1
Details of specimens for different batches of concrete.

S No	Type of concrete	Room temperature compressive strength	Thermal properties	High temperature compressive strength	High temperature tensile strength
		Specimen sizes			
		100×200 mm cylinders	100×100×300 mm prisms	75×150 mm cylinders	75×150 mm cylinders
1	SCC	12	2	18	18
2	SCC-P	12	2	18	18
3	SCC-S	12	2	18	18
4	SCC-H	12	2	18	18

specimens. Concrete prisms were used to prepare test specimens for determining thermal properties at elevated temperatures. Details of mix proportions, laboratory conditions for casting, and compressive strength results of SCC, SCC-S, SCC-P, and SCC-H are given in Table 2.

3.2. Test apparatus

3.2.1. Thermal properties

The thermal properties were measured using commercially available instruments. The specific heat, and thermal conductivity were measured using "Hot Disk TPS 2500S" thermal constant analyzer apparatus as per ISO/DIS 22007 standard [31]. This equipment was connected to a furnace in which a specimen was exposed to desired high temperature. This state-of-the-art equipment utilizes transient plane source (TPS) technique to measure thermal properties of materials from room temperature to 800 °C. A flat source sensor placed between two halves of the specimens acts like a heater (constant effect generator) and as detector (resistance thermometer) at the same time [32]. When a constant heat source is applied, the temperature in sensor rises and heat flow starts in the specimen being tested.

The test specimen must have uniform temperature distribution throughout the specimen at the time of measurement. Fig. 5 illustrates mica sensor that was placed between two specimens of concrete in the holder assembly during test. This holder assembly was further placed inside the furnace for exposure to high temperature.

For thermal expansion measurements, thermo-mechanical analysis (TMA) apparatus was used as per ASTM E 831-06 [33]. TMA utilizes a movable-core linear variable differential transducer (LVDT), which generates an output signal directly proportional to specimen dimension change. TMA can be used for measuring dimensional changes in concrete specimens from room temperature to 1000 °C. A flat-tipped standard expansion probe is placed on the concrete specimen with a small static force applied to it so that the probe stays steadily on the specimen. The specimen is subjected to temperature increase as per user defined ramp; the probe movement records the sample expansion or contraction.

3.2.2. Mechanical properties

For measuring mechanical properties, the test setup consisted of an electric furnace to heat the concrete specimens and Forney test machine to carry out strength tests (see Fig. 6). A thermal jacket was used to transfer (carry) the heated specimen to undertake compressive strength tests and an insulated steel bracket frame (see Fig. 7) was used to transfer the heated specimen to undertake splitting tensile strength tests. Forney strength test machine utilized to undertake compressive and splitting tensile strength tests is an 1800 kN load controlled compressive test machine which is capable of loading specimens up to 318 metric tons. The electric furnace used to expose specimens to high temperature was specially designed for simulating high temperature conditions and could produce maximum temperatures up to 927 °C. It is equipped with internal heating electric elements, with ramp and hold temperature controller, capable of generating different heating rates. The heating chamber of 150×200 mm internal dimensions is lined with steel jacket to withstand any possible spalling in concrete specimens.

Both thermal jacket and steel bracket frame were insulted by thermal wool that allowed transfer of heated cylinders from furnace to the strength testing machine.

3.3. Test procedure

3.3.1. Thermal properties

For undertaking thermal conductivity and specific heat measurements, test specimens of 60×60×25 mm size were prepared by slicing concrete prisms. For thermal expansion measurements, specimens of 10×10×18 mm size were sliced from concrete prisms. Thermal conductivity and specific heat of SCC and FRSCC were measured at thirteen temperature points namely 20, 100, 200, 300, 400, 450, 500, 550, 600, 650, 700, 750, and 800 °C. The smaller increments towards higher temperatures were to capture effect of phase changes in concrete on thermal properties. The age of concrete at the time of thermal property measurement tests was 6 months or older.

The SCC and FRSCC specimens were exposed to high temperature in a furnace connected to Hot Disk apparatus. Specimen and furnace temperatures were controlled by Hot Disk software. The target temperature, sensor resistance and time of measurement were controlled by programmed test set up. In each test the furnace temperature was raised to the target exposure temperature and maintained at that level till the entire test specimen reached equilibrium conditions (target temperature). At this stage the thermal conductivity and specific heat were recorded by the data acquisition system. Then the temperature in the furnace was increased to following target temperature and this procedure was continued till 800 °C.

Table 2
Mix proportions and compressive strength for different SCC mixes.

Components	SCC	SCC-S	SCC-P	SCC-H
Cement type-I ASTM C-150, kg/m^3	327	327	327	327
Fine aggregate ASTM C-33, kg/m^3	735	735	735	735
Course aggregate ASTM C-33 (maximum size 10 mm), kg/m^3	904	904	904	904
Fly ash (Class C) ASTM C-618, kg/m^3	101	101	101	101
Slag St Lawrence ASTM C-989, (Grade 120), kg/m^3	76	76	76	76
Water, kg/m^3	143	143	143	143
Water cement ratio (w/c)	0.44	0.44	0.44	0.44
Water to cementitious ratio (w/cm)	0.28	0.28	0.28	0.28
Air entraining admixture., ASTM C-260, kg/m^3	3	3	3	3
High range water reducer and plasticizer, ASTM C-494 (Type F), kg/m^3	81	81	81	81
Slump flow/spread, mm	440	410	420	410
VSI index	0.5	0.5	0.5	0.5
Humidity at casting, %	45	45	45	45
Ambient temperature at casting, °C	23	23	23	23
Concrete mix temperature at casting, °C	20	20	20	20
Steel fibers, kg/m^3	–	42	–	42
Polypropylene fibers, kg/m^3	–	–	1	1
Compressive strength, MPa				
7 days	46	48	45	46
28 days	61	57	56	57
90 days	72	70	68	72

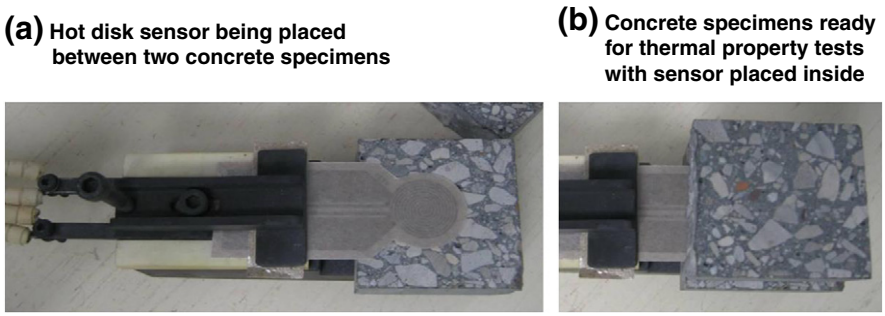

Fig. 5. Hot Disk (TPS) mica sensor being used between two specimens of concrete.

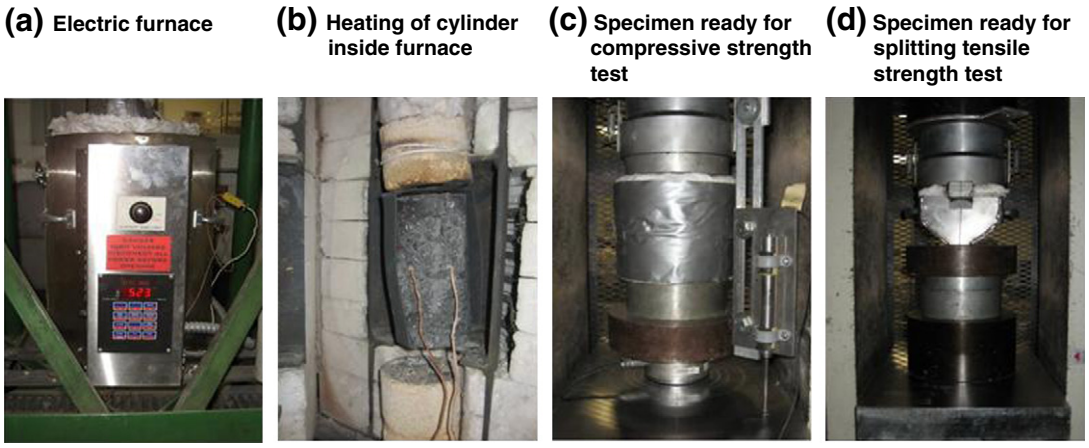

Fig. 6. Test set-up for high temperature compressive and tensile strength tests.

For thermal expansion measurements, concrete specimens prepared as per ASTM E 831-06 were placed on a pedestal in the moveable furnace of the TMA and the expansion probe was set on the specimen. The temperature increase for thermal expansion depends on the temperature ramp (heating rate) set by the user for that particular test. Once specimen was placed in position, inside TMA furnace, the test was run and controlled by software that records dimensional change with increasing temperature. For concrete specimens, the selected ramp was 5 °C per minute as per ASTM E 831-06 [33].

In order to verify reliability of measurements, thermal property tests were repeated on additional specimens from the same batch of concrete. For this, three SCC samples were selected and Hot Disk tests were repeated in the entire temperature range. The variability in the thermal conductivity and specific heat was within ±5% indicating good reliability of the measurements. To maintain the homogeneity for thermal expansion, the test specimens were carefully prepared from concrete prisms such that they contained aggregate and cement matrix in equal representative amounts. Thermal expansion test was carried out on three specimens of each SCC and FRSCC mixes for repeatability and reliability.

3.3.2. Mechanical properties

There are three steady-state test methods (conditions) to determine the high temperature strength properties of concrete, namely, residual, unstressed, or stressed test methods. These methods are well discussed by Phan [13] and Fu et al. [34], and are applicable to measure both compressive and tensile strength of concrete.

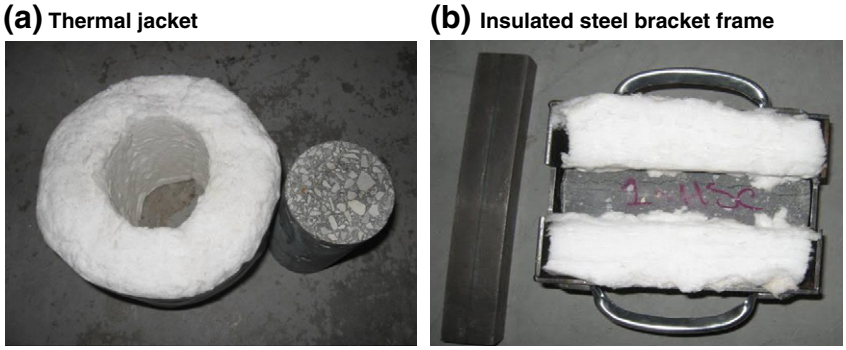

Fig. 7. Arrangements to transfer hot specimens from furnace to strength test machine.

In this study, compressive and splitting tensile strength tests were carried out at various temperatures using unstressed test method. During heating, three Type K thermocouples (TC) were used to record temperature in the furnace, at the surface and mid-depth of the cylinder. The test specimens were exposed to target temperatures of 100, 200, 400, 600, and 800 °C in an electric furnace at a heating rate of 2 °C per minute as proposed by RILEM [35] test procedure. When the target temperature was attained in the furnace, the cylinder continued to be maintained at this temperature (in the furnace) for 2 h till desired steady state condition was reached throughout the specimen.

Fig. 8 illustrates the temperature development in the furnace, on the surface and at the center of 75×150 mm SCC cylinder for the case of 600 °C target temperature. As expected, the rise in temperature at the center of the specimen was much slower than the surface and furnace temperature and this is due to low thermal conductivity of concrete. It was observed that a hold time of 2 h was required to reach the steady state (uniform temperature distribution) in specimen at all target temperatures.

After achieving steady state condition in cylinders inside the furnace, the hot cylinders were taken out from the furnace, were covered by thermal jacket for compressive strength and in steel bracket frame for splitting tensile strength testing apparatus. As no specific test procedure for high temperature compressive and tensile tests is available, ASTM C 39 and ASTM C 496 procedures specified for room temperature compressive and tensile strength test, were used for high temperature strength tests. Once the thermally insulated specimen was transferred for compressive or tensile strength test, an average drop of 10 °C was observed in the specimens from start to end of the strength test, well within the RILEM [35] recommendations. The specimen in each test was loaded in prescribed increments till failure of cylinder and failure load was recorded. For both compressive and splitting tensile strength tests, one specimen was tested at each target temperature. Additional tests were done for repeatability to reconfirm the doubtful results.

4. Results and discussion

4.1. Thermal properties

4.1.1. Thermal conductivity

The measured thermal conductivity of SCC and FRSCC are plotted in Fig. 9 as a function of temperature. Thermal conductivity of four types of SCC ranges between 2.8 and 3.6 W/m-°C at room temperature. This higher thermal conductivity of SCC as compared to HSC at room temperature is attributed to high ratio of paste content and admixtures in SCC [36]. For all concretes, thermal conductivity initially decreases with temperature up to 400 °C, and then it increases marginally between 400 and 500 °C, and finally decreases again up to 800 °C. This trend in thermal conductivity can be attributed to variation of moisture content with increase in temperature [10]. The initial steep slope of thermal conductivity up to 400 °C can be attributed to moisture loss at a faster pace resulting from the evaporation of free and pore water in concrete with rise in temperature. The minor variation in thermal conductivity between 400 °C and 500 °C is probably due to breakdown of $Ca(OH)_2$ into CaO and H_2O, which increases moisture resulting in small increase in thermal conductivity. Beyond 500 °C, there is slow decrease in thermal conductivity due to liberation of small amount of strongly held moisture left within calcium silicate hydrate (C-S-H) layers. Thermal conductivity of all SCC concretes follows quite similar trend and lie closer to 0.6 W/m-°C band difference and therefore it is deduced that there is not much significant variation in thermal conductivity of SCC and FRSCC throughout the temperature (20–800 °C) range. Loss of thermal conductivity observed for SCC is similar in trends to HSC as reported by Kodur and Khaliq [14]. However, SCC has higher conductivity as compared to HSC, and this might be attributed to the fact that SCC is produced by excessive use of chemical admixtures, and thus it has increased amount dissolved chemical ions in mixed water.

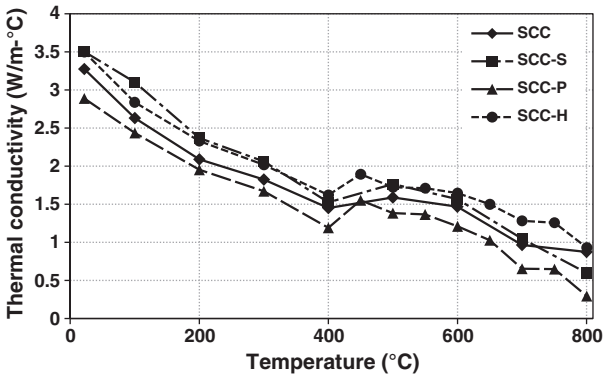

Fig. 9. Measured thermal conductivity of SCC and FRSCC as a function of temperature.

4.1.2. Specific heat

The variation of specific heat for SCC and FRSCC with temperature is illustrated in Fig. 10. The specific heat for SCC is almost constant between 20 and 400 °C and increases up to 700 °C, finally becoming constant again between 700 and 800 °C. Specific heat of FRSCC also remains almost constant up to 400 °C, then increases up to about 650 °C and finally scatters out in 650–800 °C range as a result of

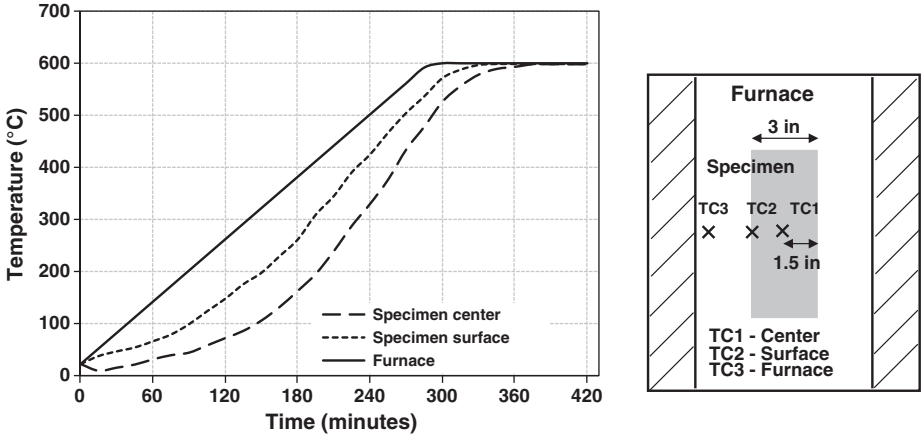

Fig. 8. Heating characteristics of specimen at 600 °C.

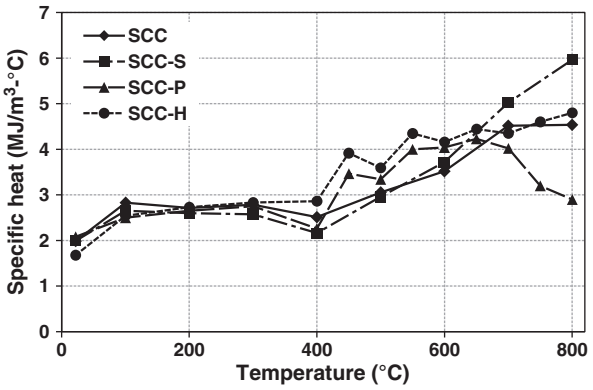

Fig. 10. Measured specific heat of SCC and FRSCC as a function of temperature.

presence of different fibers. SCC-S and SCC-H exhibit slightly higher values of specific heat in 650–800 °C temperature range that may be attributed to presence of steel fibers. Use of polypropylene fibers reduces the specific heat between 650 and 800 °C. This can be attributed to less heat required to raise the temperature of pervious SCC-P resulting from burning of polypropylene fibers. Moreover, the deterioration of concrete between 650 and 800 °C temperatures, resulting in micro and macro crack development will also add to porosity of SCC-P. SCC-S has the highest specific heat between 650 and 800 °C temperatures; however SCC-H has lower specific heat, which again can be attributed to presence of propylene fibers. This is further proved by the fact that SCC-P has the lowest specific heat between 650 and 800 °C temperature range. This can be attributed to the lower permeability and dense microstructure of SCC that requires extra heat to convert moisture into vapors. SCC displayed higher specific heat values as compared to specific heat of HSC as reported in literature [14].

4.1.3. Thermal expansion

The variation of thermal expansion of SCC and FRSCC is plotted as a function of temperature in Fig. 11. Thermal expansion of SCC increases between 20 and 600 °C becomes constant between 600 and 800 °C, then again increases up to 1000 °C. Thermal expansion generally increases with temperature for FRSCC, this increase is substantial in 20–600 °C temperature range, and is mainly due to high thermal expansion resulting from constituent aggregates and cement paste in concrete. The expansion rate for all concretes reduces between 600 and 800 °C, but increases again above 800 °C. The decrease in thermal expansion in 600–800 °C range can be attributed to dissociation of calcium carbonate [37] and the increase in expansion above 800 °C is attributed to decomposition of concrete due to complete dehydration and excessive micro and macro crack development [38].

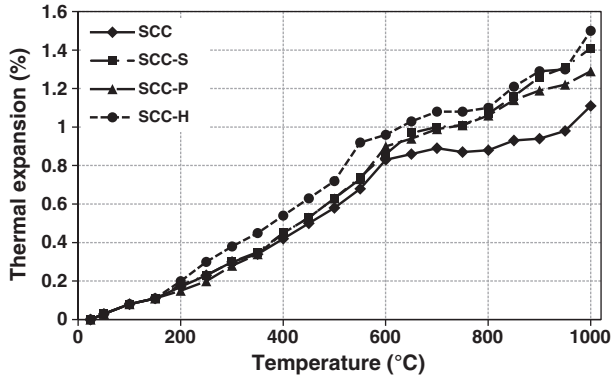

Fig. 11. Measured thermal expansion of SCC and FRSCC as a function of temperature.

Thermal expansion of FRSCC in 600–1000 °C range is higher than SCC; and is the highest in SCC-S and SCC-H mixes; this can be attributed to presence of steel fibers since steel fibers arrest progression of cracks. Overall, there is not a wide difference between thermal expansions of different FRSCC types.

4.2. Mechanical properties

4.2.1. Compressive strength

The recorded applied load at which the heated cylinder failed in compression was used to compute compressive strength at each temperature and these values are plotted as a function of temperature for SCC and FRSCC in Fig. 12(a). In all four concretes, physical and chemical changes that occur at higher temperatures lead to significant reduction in compressive strength. For SCC, there is reduction in compressive strength at 100 °C initially and then strength regain at 200 °C. The strength loss till 100 °C can be attributed to initial moisture loss in SCC. The increase in strength in 100–200 °C temperature range can be attributed to rehydration and moisture migration [17,18]. SCC displayed higher compressive strength as compared to FRSCC. Liu et al. [6] have reported that gas permeability of polypropylene fiber reinforced SCC increases at elevated temperatures due to increase in pore size and their connectivity. The higher compressive strength of SCC is therefore attributed to dense microstructure of SCC as compared to FRSCC. In the case of FRSCC the loss of compressive strength with temperature is about same throughout temperature range. This can be deduced that the addition of fibers does not have much effect on the variation of compressive strength of SCC with temperature.

It has been established that moisture in concrete has significant effect on high temperature compressive strength of concrete [39]. For initial moisture loss up to 100 °C, due to evaporation of free water, the strength drops sharply; however, with loss of free water, compressive strength stabilizes at temperatures between 100 and 400 °C. Beyond 400 °C the strength loss becomes gradual with increase in temperature for SCC and FRSCC. This gradual degradation of strength (without substantial drop) can be attributed to slow loss of chemically bound water due to dehydration and disintegration of C-S-H in concrete [37].

The ratio of recorded compressive strength at target temperature ($f'_{c,T}$) to compressive strength at room temperature (f'_c) for SCC and FRSCC is shown in Fig. 12(b). The relative strength loss in all concretes follows similar trend to its absolute strength. There is noticeable strength retention in all SCC and FRSCC even at 800 °C and this ranges from 30 to 44%. This level of strength retention is much higher than conventional HSC, which has less than 20% relative compressive strength at 800 °C [40,41]. This observation confirms that high strength SCC has superior microstructure and therefore displays better compressive strength even at higher temperatures.

4.2.2. Splitting tensile strength

The recorded applied load at which the heated cylinder split in tension was used to compute splitting tensile strength at each temperature and this is plotted for SCC and FRSCC as a function of temperature in Fig. 13(a). All four concretes experienced loss in splitting tensile strength with temperature. In the case of SCC which has a lower tensile strength of 4 MPa at room temperature, the reduction in tensile strength is gradual and almost linear up to 400 °C and then there is sharp reduction in tensile strength to 800 °C. This sharp reduction in splitting tensile strength beyond 400 °C can be attributed to the development of excessive micro and macro cracks resulting from thermal stresses and thermal incompatibility within SCC. This conforms to the sharp loss to splitting tensile strength reported by Sideris [5], Chan [19] and Khoury [24].The slower degradation of strength (without substantial changes) at early stages in all SCC's can be attributed to its higher stiffness as compared to FRSCC. Both SCC-S and SCC-H display higher ratio of splitting tensile strength in 300–800 °C temperatures range which can

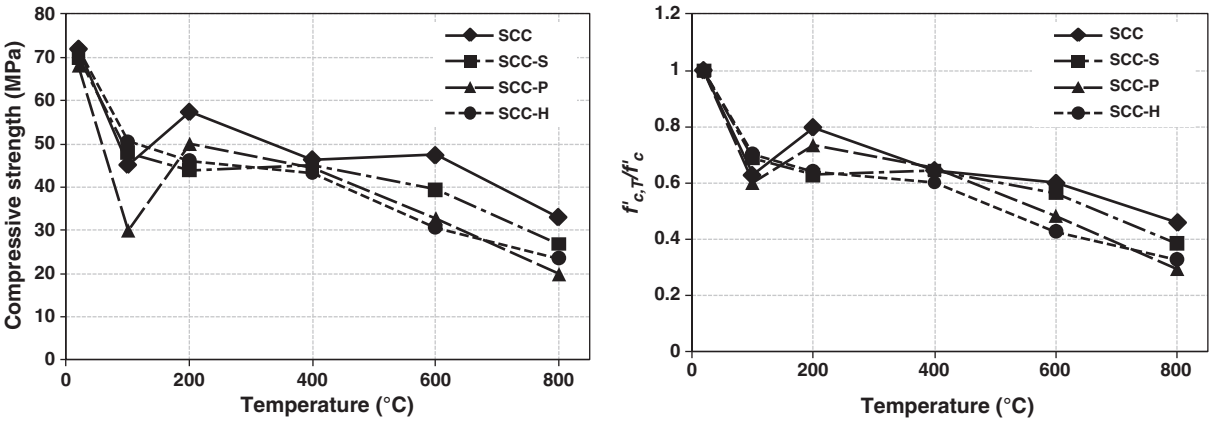

Fig. 12. Compressive strength of SCC and FRSCC as function of temperature.

be attributed to presence of steel fibers. SCC-P has the lowest splitting tensile strength beyond 250 °C which indicates that after melting of polypropylene fibers at about 180 °C there is significant degradation in its microstructure resulting from increased porosity.

Fig. 13(b) illustrates the ratio of recorded splitting tensile strength at target temperature ($f'_{t,T}$) to splitting tensile strength at room temperature (f'_t) for SCC and FRSCC. The ratio plotted in these figures indicates that addition of polypropylene fibers to SCC reduced its splitting tensile strength as both SCC-P and SCC-H display reduction in tensile strength ratio. This reduced splitting tensile strength could be attributed to the increased porosity in SCC due to melting of polypropylene fibers inside FRSCC which results in weak microstructure. Test data indicates that SCC and FRSCC, have about 40–50% $f'_{t,T}/f'_t$ at 600 °C that is quite significant.

The improved tensile strength in FRSCC is similar to the fire behavior of fiber reinforce HSC reported by Khaliq and Kodur [42]. Tensile strength of steel fiber reinforced HSC was significantly higher, which was attributed to effectiveness of steel fibers in bridging the cracks under tensile loading. It can be seen in case of SCC as well that steel fibers are effective to enhance the tensile strength especially up to 400 °C and this enhanced f'_t is beneficial in mitigating the fire induced spalling.

4.2.3. Elastic modulus

Data generated from compressive stress–strain curves was used to obtain elastic modulus of SCC and FRSCC at various temperatures. Fig. 14 illustrates the relative elastic modulus ($E_{c,T}/E_c$) and FRSCC as a function of temperature. The trends show that modulus for all four concretes decrease in 20–800 °C temperature range. SCC displays lower elastic modulus of all concretes which can be attributed to stiff and dense microstructure of SCC as compared to FRSCC resulting in excessive deterioration due to thermal stresses. This reduction in elastic modulus for SCC is the same as reported by Persson [7] and Bamonte and Gambarova [23]. However, the ratio of reduction for elastic modulus of FRSCC is much less compared to SCC. This proves the fact that addition of different fibers to SCC enhances its elastic modulus at higher temperatures.

Modulus for SCC-S and SCC-H initially remains constant up to 100 °C and then sharply reduces up to 200 °C before gradual decay in the temperature range of 200–800 °C. The higher modulus observed in SCC-S and SCC-H can be attributed to increased ductility due to the presence of steel fibers which act as crack arresters as these provide necessary bond against development of cracks. The observed modulus of SCC and SCC-P is lower in comparison to SCC-S and SCC-H throughout 20–800 °C temperature range. The addition of polypropylene fibers shows improved modulus in 20–800 °C temperature range, in comparison to SCC. This improvement in modulus is marginal in 20–200 °C, but further enhances above 200 °C, after melting of polypropylene fibers (around 170 °C) that increases porosity. This can be attributed to less deterioration in SCC-P in comparison SCC that undergoes higher thermal deterioration due to dense microstructure.

It should be noted that the above presented strength and modulus trends are applicable for material characterization of SCC under test conditions used in this program. Factors such as heating and specimen size can have some influence on the exact values at a given temperature, but the general trends are likely to follow similar trends as in this study.

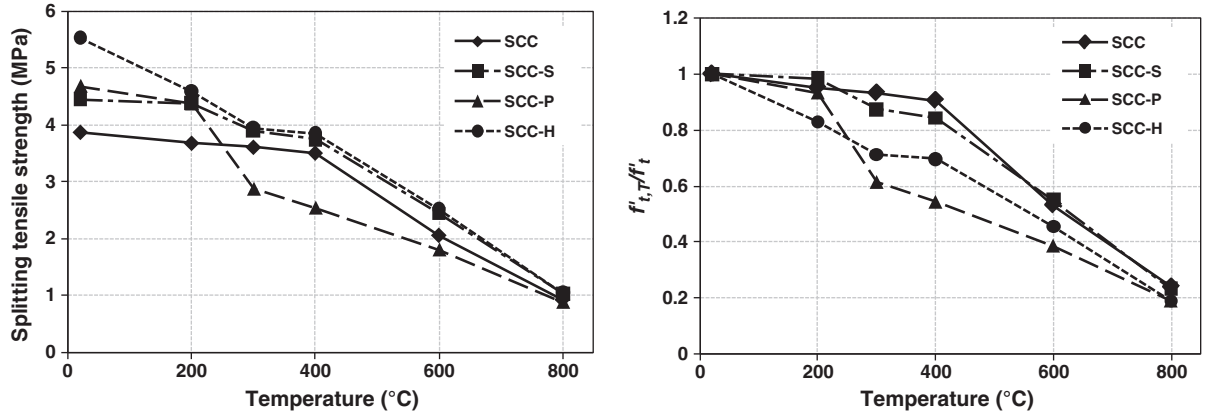

Fig. 13. Splitting tensile strength of SCC and FRSCC as function temperature.

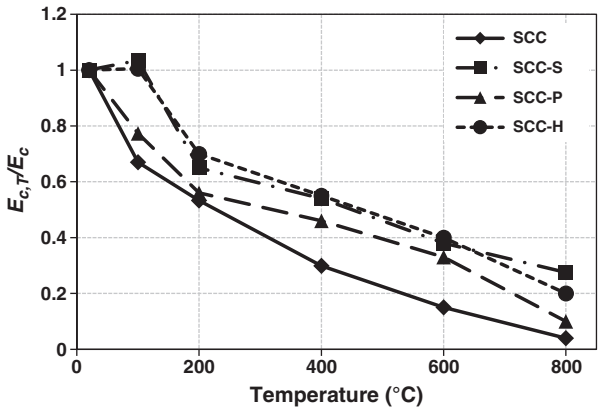

Fig. 14. Relative elastic modulus of different SCC and FRSCC as function of temperature.

5. High temperature property relationships

Data generated from the thermal and mechanical property measurements was utilized to develop thermal and mechanical property relationships for SCC and FRSCC. These properties are expressed in the form of empirical relationships over temperature range of 20–800 °C for thermal conductivity and specific heat and 20–1000 °C for thermal expansion. Relations for mechanical properties of SCC and FRSCC include compressive strength, tensile strength and elastic modulus in 20–800 °C temperature range. These empirical relationships were arrived at based on linear regression analysis. For the regression analysis, measured thermal and mechanical properties were used as response parameter with temperature as their predictor parameter. Commercially available statistical software (Minitab) was used to find a linear fit through regression analysis. The accuracy of the statistical model is represented by coefficient of determination 'R^2', that represents proportion of the sum of squares of deviations of the response values about their predictor [43]. The value of R^2 varies between 0 and 1, where 1 is the perfect fit of the equation to underlying data. The R^2 value obtained for the proposed equations lies between 0.82 and 0.99 for thermal properties and 0.9 and 0.96 for mechanical properties, which represents a reasonably high confidence level in light of high variability in concrete properties.

5.1. Thermal properties

As shown by test data, it is evident that thermal properties are primarily a function of temperature. To reflect this trend separate expressions are developed for thermal conductivity (k_t), specific heat (c_P) and thermal expansion (ε_{th}) of SCC and FRSCC. When the property trends are similar, one representative relationship is given for both SCC and FRSCC types. For SCC types having significant variation in the property, a separate relationship is presented. These relations are valid for SCC and FRSCC in 20 to 800 °C temperature range for all thermal (thermal conductivity and specific heat) and mechanical properties (compressive, splitting tensile strength and elastic modulus). For thermal expansion the relations are valid in 20 to 1000 °C temperature range. These thermal property relations are presented in different temperature ranges in Table 3.

5.2. Mechanical properties

The variation of compressive strength ($f'_{c,T}$), tensile strength ($f'_{t,T}$) and elastic modulus $E_{c,T}$ with temperature can be related through a coefficient β_T representing ratio of respective strength at target temperature to that at room temperature (f'_c, f_t *and* E_c) given in Table 3. Due to least difference in variation in high temperature compressive strength of SCC and FRSCC, single representative relation is presented for $f'_{c,T}$. However, because of significant difference in variation of high temperature splitting tensile strength and elastic modulus, separate relationships are presented for SCC and FRSCC.

$$\beta_{T,compressive} = \frac{f'_{c,T}}{f'_c} \tag{1}$$

$$\beta_{T,tensile} = \frac{f'_{t,T}}{f'_t} \tag{2}$$

$$\beta_{T,modulus} = \frac{E_{c,T}}{E_c} \tag{3}$$

The value of β_T for respective mechanical property at different temperatures can be obtained from equations in Table 3 for SCC and FRSCC. In lieu of equations, reduction factor β_T, at different temper-

Table 3
High temperature property relationships for thermal and mechanical properties of SCC and FRSCC.

Property	Concrete type	Relation
Thermal conductivity (W/m-°C)	SCC, SCC-P, SCC-S and SCC-H	$k_t = \begin{Bmatrix} 3.12-0.0045T & 20°C \le T \le 400°C \\ 3-0.0025T & 400°C \le T \le 800°C \end{Bmatrix}$
Specific heat (MJ/m^3-°C)	SCC, SCC-S and SCC-H	$c_p = \begin{Bmatrix} 2.4+0.001T & 20°C \le T \le 400°C \\ 0.6-0.006T & 400°C \le T \le 800°C \end{Bmatrix}$
Specific heat (MJ/m^3-°C)	SCC-P	$c_p = \begin{Bmatrix} 2.4+0.001T & 20°C \le T \le 400°C \\ 0.6-0.006T & 400°C \le T \le Tb650°C \\ 10.6-0.01T & 650°C \le T \le 800°C \end{Bmatrix}$
Thermal expansion (%)	SCC, SCC-P, SCC-S and SCC-H	$\varepsilon_{th} = \begin{Bmatrix} 0 & 20°C \\ -0.1+0.0015T & 20°C bT \le 800°C \end{Bmatrix}$
Compressive strength	SCC, SCC-P, SCC-S and SCC-H	$\beta_T, compression = \begin{Bmatrix} 1.0 & 20°C \\ 0.99-0.002T & 100°C \le Tb200°C \\ 0.73-0.0005T & 200°C \le T \le 800°C \end{Bmatrix}$
Splitting tensile strength	SCC and SCC-P	$\beta_T, tensile = \begin{Bmatrix} 1.0 & 20°C \\ 0.99-0.001T & 100°C \le T \le 800°C \end{Bmatrix}$
Splitting tensile strength	SCC-S and SCC-H	$\beta_T, tensile = \begin{Bmatrix} 1.0 & 20°C \\ 1.1-0.001T & 100°C \le Tb800°C \end{Bmatrix}$
Elastic modulus	SCC and SCC-P	$\beta_T, modulus = \begin{Bmatrix} 1.0 & 20°C \\ 0.84-0.001T & 100°C \le T \le 800°C \end{Bmatrix}$
Elastic modulus	SCC-S and SCC-H	$\beta_T, modulus = \begin{Bmatrix} 1.0 & 20°C \\ 1.1-0.002T & 100°C \le Tb200°C \\ 0.88-0.008T & 200°C \le Tb800°C \end{Bmatrix}$

Table 4
Compressive strength, tensile strength and elastic modulus reduction factor β_T at different temperatures for SCC and FRSCC.

Temperature — °C	Reduction factor (β_T)				
	Compressive strength	Tensile strength		Elastic modulus	
	SCC and FRSCC	SCC-P	SCC, SCC-S, SCC-H	SCC and SCC-P	SCC-S and SCC-H
20	1	1	1	1	1
100	0.79	0.89	0.95	0.74	0.9
200	0.59	0.79	0.9	0.64	0.72
300	0.56	0.69	0.8	0.54	0.64
400	0.53	0.59	0.7	0.44	0.56
600	0.43	0.39	0.5	0.34	0.4
800	0.33	0.19	0.3	0.04	0.24

atures can be used for evaluating compressive and tensile strength and elastic modulus for SCC and FRSCC as given in Table 4.

6. Conclusions

Based on the studies presented in this paper, the following conclusions are drawn:

- Temperature has significant influence on thermal conductivity, specific heat and thermal expansion of SCC and FRSCC. The thermal conductivity generally decreases with temperature, while the thermal expansion increases with temperature up to 800 °C. However, specific heat remains almost constant up to about 400 °C, and then increases with presence of steel fibers.
- Addition of steel, polypropylene, and hybrid fibers to SCC does not significantly alter the thermal conductivity throughout 20–800 °C temperature range.
- SCC and FRSCC experience significant expansion with temperature; SCC has the lowest thermal expansion whereas SCC with hybrid fibers has the highest thermal expansion.
- Addition of steel, polypropylene, and hybrid fibers does not have much effect on high temperature compressive strength of SCC.
- Steel fibers improve tensile strength of SCC-S up to 400 °C which can be beneficial to minimize fire induced spalling. Addition of polypropylene fibers reduces the tensile strength of SCC-P and SCC-H at higher temperature.
- Addition of fibers improves the modulus of SCC; steel fibers significantly enhance the elastic modulus of FRSCC.
- The proposed relationships for high temperature thermal and mechanical properties can be used as input data in computer programs for evaluating the fire response of SCC and FRSCC structures exposed to fire.

Acknowledgments

The research presented in this paper is supported by the National Science Foundation CMMI program (Grant No. CMMI 0601178) and Michigan State University through Strategic Partnership Grant (No. 71-4434). Any opinions, findings, and conclusions or recommendations expressed in this paper are those of the authors and do not necessarily reflect the views of the sponsors.

References

[1] A. Noumowé, H. Carré, A. Daoud, H. Toutanji, High-strength self-compacting concrete exposed to fire test, J. Mater. Civ. Eng. ASCE 18 (2006) 754–758.
[2] V.R. Kodur, F.P. Cheng, T.C. Wang, M.A. Sultan, Effect of strength and fiber reinforcement on the fire resistance of high strength concrete columns, J. Struct. Eng. ASCE 129 (2003) 253–259.
[3] L.T. Phan, N.J. Carino, Review of mechanical properties of HSC at elevated temperature, J. Mater. Civ. Eng. ASCE 10 (1998) 58–64.
[4] V.R. Kodur, Spalling in high strength concrete exposed to fire — concerns, causes, critical parameters, and cures, Proceedings of the ASCE Structures Congress, 2000, pp. 1–9, (Philadelphia, PA).
[5] K.K. Sideris, Mechanical characteristics of self-consolidating concrete exposed to elevated temeperatures, ASCE J. Mater. Civ. Eng. 19 (2007) 648–654.
[6] X. Liu, G. Ye, G. De Schutter, Y. Yuan, L. Taerwe, On the mechanism of polypropylene fibres in preventing fire spalling in self-compacting and high-performance cement paste, Cem. Concr. Res. 38 (2008) 487–499.
[7] B. Persson, Fire resistance of self-compacting concrete, SCC Mater. Struct. 37 (2004) 575–584.
[8] T.T. Lie, Structural fire protection, ASCE Committee on Fire Protection, Structural Division, American Society of Civil Engineers, New York,NY, 1992, pp. 225–229.
[9] K.Y. Shin, S. Kim, J. Kim, M. Chung, P. Jung, Thermo-physical properties and transient heat transfer of concrete at elevated temperatures, Nucl. Eng. Des. 212 (2002) 233–241.
[10] Z.P. Bazant, M.F. Kaplan, Concrete at Temperatures: Material Properties and Mathematical Models, Longman Group Limited, Essex, England, 1996.
[11] T.Z. Harmathy, L.W. Allen, Thermal properties of selected masonry unit concretes, ACI J. Proc. 70 (1973) 132–142.
[12] V.R. Kodur, M.A. Sultan, Structural behaviour of high strength concrete columns exposed to fire, Proceedings, Int Symposium on High Performance and Reactive Powder Concrete, Sherbrooke, Canada, 1998, pp. 217–232.
[13] L.T. Phan, Fire Performance of High-strength Concrete: A Report of the State-of-the-art, National Institute of Standards and Technology, Gaithersburg, Md, USA, 1996.
[14] V.K.R. Kodur, W. Khaliq, Effect of temperature on thermal properties of different types of high strength concrete, Journal of Materials in Civil Engineering, ASCE, In Print, 2011.
[15] T. Uygunoğlu, B. Topçu, Thermal expansion of self-consolidating normal and lightweight aggregate concrete at elevated temperatures, Constr. Build. Mater. 23 (2009) 3063–3069.
[16] P.K. Mehta, P.J.M. Monteiro, Concrete: Microstructure, Properties, and Materials, 3rd ed., The McGraw-Hill Companies, Inc., New York, USA, 2006.
[17] H. Fares, S. Remond, A. Noumuwe, A. Cousture, High temperature behaviour of self-consolidating concrete microstructure and physicochemical properties, Cem. Concr. Res. 40 (2010) 488–496.
[18] W.P.S. Dias, G.A. Khoury, P.J.E. Sullivan, Mechanical properties of hardened cement paste exposed to temperaures up to 700 °C, ACI Mater. J. 87 (1990) 160–166.
[19] Y.N. Chan, G.F. Peng, M. Anson, Residual strength and pore structure of high-strength concrete and normal strength concrete after exposure to high temperatures, Cem. Concr. Compos. 21 (1999) 23–27.
[20] S.P. Shah, Do fibers increase the tensile strength of cement-based matrixes? ACI Mater. J. 88 (1991) 595–602.
[21] F. Ali, A. Nadjai, G. Silcock, A. Abu-Tair, Outcomes of a major research on fire resistance of concrete columns, Fire Saf. J. 39 (2004) 433–445.
[22] F. Ali, Is high strength concrete more susceptible to explosive spalling than normal strength concrete in fire? Fire Mater. 26 (2002) 127–130.
[23] P. Bamonte, G. Gambarova, High-temperature Resistance of Self-consolidating Concrete, ACI Spring Convention 2010, Chicago, USA, 2010.
[24] G.A. Khoury, Compressive strength of concrete at high temperatures: a reassessment, Mag. Concr. Res. 44 (1992) 291–309.
[25] B. Perrson, Fire resistance of self-compacting concrete, SCC, Mater. Struct. 37 (2004) 575–584.
[26] V.R. Kodur, R. McGrath, Fire endurance of high strength concrete columns, NRCC-45141, National Research Council Canada, 2003, pp. 1–13.
[27] P. Kalifa, G. Chéné, C. Gallé, High-temperature behavior of HPC with polypropylene fibers from spalling to microstructure, Cem. Concr. Res. 31 (2001) 1487–1499.
[28] V.R. Kodur, Fiber reinforced concrete for enhancing structural fire resistance of columns, American Concrete Institute, 1999, pp. 215–234, (SP 182-12).
[29] F. Ali, A. Nadjai, , (SP-255-9), Fire Resistance of Concrete Columns Containing Polypropylene and Steel Fibers, ACI Special Publication, 255, 2008, pp. 199–216.
[30] N. Anagnostopoulos, K.K. Sideris, A. Georgiadis, Mechanical characteristics of self-compacting concretes with different filler materials exposed to elevated temperatures, Mater. Struct. 42 (2009) 1393–1405.
[31] ISO/DIS22007-2:2008, Determination of thermal conductivity and thermal diffusivity, Part 2: Transient Plane Heat Source (Hot Disc) Method, ISO, Geneva, Switzerland, 2008.
[32] B. Adl-Zarrabi, L. Boström, U. Wickström, Using the TPS method for determining the thermal properties of concrete and wood at elevated temperature, Fire and Mater. 30 (2006) 359–369.
[33] ASTM Standard E831, Standard Test Method for Linear Thermal Expansion of Solid Materials by Thermomechanical Analysis, ASTM International, West Conshohocken, PA, 2006.
[34] Y.F. Fu, Y.L. Wong, C.S. Poon, C.A. Tang, Stress–strain behaviour of high-strength concrete at elevated temperatures, Mag. Concr. Res. 57 (2005) 535–544.
[35] T.C. Rilem, 129-MHT, test methods for mechanical properties of concrete at high temperatures, Part 4 — tensile strength for service and accident conditions, Mater. Struct. 33 (2000) 219–223.
[36] I.B. Topçu, T. Uygunoğlu, Effect of aggregate type on properties of hardened self-consolidating lightweight concrete, Constr. Build. Mater. 24 (2010) 1286–1295.
[37] FIB Bulletin 38, Fire design of concrete structures — materials, structures and modelling, The International Federation for Structural Concrete (fib — fédération internationale du béton), 2007 (Switzerland).

[38] Y.F. Fu, Y.L. Wong, C.S. Poon, C.A. Tang, P. Lin, Experimental study of micro/macro crack development and stress–strain relations of cement-based composite materials at elevated temperatures, Cem. Concr. Res. 34 (2004) 789–797.
[39] C. Castillo, A.J. Durrani, Effect of transient high temperature on high strength concrete, ACI Mater. J. 87 (1990) 47–53.
[40] B. Chen, J. Liu, Residual strength of hybrid-fiber-reinforced high-strength concrete after exposure to high temperatures, Cem. Concr. Res. 34 (2004) 1065–1069.
[41] R. Felicetti, P.G. Gambarova, Effects of high temperature on the residual compressive strength of high-strength siliceous concretes, ACI Mater. J. 95 (1998) 395–406.
[42] W. Khaliq, V. Kodur, High Temperature Properties of Fiber Reinforced High Strength Concrete, Innovations in Fire Design of Concrete Structures — ACI SP, 279, 2011, (3–1 3–42).
[43] W. Mendenhall, T. Sincich, Statistics for Engineering and the Sciences, 5th ed., Prentice Hall, New Jersey, USA, 2007.